ICAS-88-4.3.3

FLOW PROPERTIES ASSOCIATED WITH WING/BODY JUNCTIONS IN WIND TUNNEL AND FLIGHT

A. Bertelrud
FFA , The Aeronautical Research Institute of Sweden
S-161 11 BROMMA, Sweden

J. Szodruch
MBB-UT, Bremen , West Germany

and
J. Olsson
FFA, The Aeronautical Research Institute of Sweden
S-161 11 BROMMA, Sweden

SUMMARY

The complex flow occurring in the wing/body junction of aircraft , i.e. in the pod/wing junction or the pod/nacelle junction , has been identified as a source of drag increase in most cases. While attached boundary layers (three- as well as two-dimensional) are becoming commonplace to compute with various types of boundary layer codes , it is not yet clear how to do a proper modelling for a computational prediction of this type of flow. In the present paper experimental data is presented concerning three-dimensional time-averaged and turbulence data obtained within the junction during flight tests , and from the wake region in a wind tunnel test.

FAIRING DESIGN ON TRANSPORT AIRCRAFT

Despite the present low fuel prices aerodynamic performance of commercial transport aircraft influences the Direct Operating Cost (DOC) considerably (between 40 % and 10 % depending on aircraft size and range). Thus it is important not only to improve the aerodynamic standard on a large scale by introducing advanced technologies, but also to look at local flow phenomena in order to continuously advance the aircraft performance. One example of these continuous improvement programs is the modification of the contour of aircraft parts and fairings.

Looking at a modern transport aircraft there are fairings or fillets in all kind of body junctions, i.e. fuselage/wing , fuselage/elevator, wing/pylon, see Figure 1. The past experience in aircraft programs has shown potential drag savings at cruise conditions of about 0.5 % when modifying either wing/pylon fairings or fillets at the tailplane root. The wing/fuselage fairing offers even larger drag reduction potential. As is sketched in Figure 2 the different fairings between Airbus A300 and A310 can lead to interference drag improvements of up to 2 % of total aircraft drag [1]. This drag reduction potential justifies more detailed flow field investigations but also requires new or industrially adapted measuring techniques for wind tunnel and free flight conditions [2].

In the following we shall concentrate on some design aspects and measurements on wing/fuselage fairings. The leading edge radius at the wing root is an important parameter for the fairing design since a relatively blunt nose can result in boundary layer separation in the wing/fuselage junction and induce increased drag. Then the aim of introducing the fairing is to reduce the high flow velocities over the wing root section, as is demonstrated in Figure 3 [3]. Thus the fillet size depends on relative root thickness, leading edge radius, and wing position at fuselage, i.e. setting angle and vertical location. In the example it can be seen how the fillet finally has to match the corresponding pressure distribution in order to minimize the drag. This was confirmed by wind tunnel tests at cruise speed. Figure 4 shows the drag polar for three configurations, small fillet, large fillet and without any fairing.The pressure distribution of the research wing was of the type as sketched on the right side of Figure 3, so it is seen that already a small fillet is sufficient to improve drag by about 5 counts [3]. Final fairing design for the aircraft is based on computations and wind tunnel experiment. Even with relatively conventional CFD-methods (like a coupled vortex lattice/boundary layer code) first answers are achieved. The comparison with the experiment is in first approximation sufficient for the designer. As an example Figure 5 shows theoretical and experimental pressure distributions in the fuselage/wing junction of a typical transport aircraft [4]. More sophisticated numerical methods are available as recently reported in [5],however they are certainly more time-consuming and the experimental validation has not been demonstated.

Two oil-flow visualizations are presented in Figure 6 where favourable and unfavourable fairing designs can be recognized from wall shear directions. The upper figure shows that at the stagnation point the intersection fuselage/fillet is more on the lower side so that there is a strong flow around the leading edge with all the before mentioned consequences. The oil flows in the lower picture demonstrates the result of a good fillet design. The leading edge of the fairing is drooped considerably resulting in a smooth pressure distribution and wall shear directions even at lift conditions.

BACKGROUND

While the fairing design has to be done by all aircraft manufacturers, few aircraft or aircraft models have been thoroughly investigated concerning local flow patterns. To some extent this is a result of common practice; the fuselage and wings are designed separately or put together in the initial design. while the fairing is hard to model and analyze. It is therefore subject to trial and error after the basic design has been frozen. Also , apart from the generalizations concerning effects of leading edge and junction radii, the complex geometry makes it hard to adapt lessons from one aircraft project to another.
The analysis of flow along simplified corners,i.e. in general 90 deg. sharp corners, ducted flows or schematic wings on flat plates is often performed in low Reynolds number facilities.
The past few years several investigations have been performed under laboratory conditions to describe wing-body junction flows experimentally or computationally. In the general case vorticity from the boundary layer of the fuselage, interacts with the wing leading edge, and single or multiple skew-induced vortices are formed. This is an interaction of the "first" kind, in contrast to the Reynolds-stress induced vortices common in channel flows. In most experiments the development of the vortices downstream is then monitored through an idealized junction, generally a right angle corner with zero streamwise pressure gradient. This creates a flow which may not be representative of practical cases, which in general has a much higher Reynolds number , are filleted and a considerable streamwise pressure gradient.

There are several parameters characterizing the flow:
- laminar, transitional or turbulent
- streamwise pressure gradient
- relative thickness of the shear layers in the corners
- leading edge shape; i.e. filleted , straight or swept
- shape of the second surface; flat with elliptical, sharp or profiled leading edge or profiled throughout.
- filleting in the junction itself

For a practical case it is also essential to know what happens to the vortices as they merge into the wake behind the wing/body junction. This requires a comprehensive survey in the flowfield to determine the three-dimensional distributions of velocity as well as vorticity.

A vast number of experiments have been performed in channel flow , but as they belong to a different flow category , they have not been included here. Bradshaw has characterized the different types of 'complex' flows in a couple of papers [6 , 7]. Based on experiments by Parr , Gersten [8] made rule-of-thumb correlations for use in a laminar, transitional as well as turbulent flat plate corner flow, i.e. with zero pressure gradient.
He noted that transition to turbulent flow occured much earlier than for a flat plate alone, and introduced an interference displacement thickness and interference skin friction to describe the corner interaction; see Figure 7. One may note that the main effect of the corner as long as the flow is laminar , is to reduce the skin friction (Carrier [9]), while secondary flow occurs in the turbulent case causing an increase. Carrier in his analysis neglected the streamwise vorticity, but this has since been included [10]. Gersten also included pressure gradient effects in terms of the Euler number: Eu = (dp/dx)/(ro*U^2), obtained with a constant Euler number flow. Figure 8 shows the displacement thickness for flat plate flow (subscript 2) and the interference displacement thickness (subscript 3) defined earlier.
Bragg [11] did extensive measurements of the turbulent flow in the corner of two flat plates at zero as well as an adverse pressure gradient approach separation , and developed formulae for the distribution of wall shear stresss and the extent of the interaction region as determined from the wall shear distribution.
Over several years the group at Queen Mary College performed a series of experiments into the different aspects of corner flow. Young [11] has given a review of the work , and some of the features will be mentioned here.

Zamir and Young [13, 14] made experiments with laminar flow in a 90 degree corner set at different angles of attack. They documented the flow going to transition and separation , and suggested criteria for the flow. Barclay [15] did a similar experiment, but with a 135 degree corner angle. Later Mojola [16,17] investigated the turbulent flow in the 90 degree corner. So far the investigations had been concentrated on the corner itself , giving moderate attention to the leading edge. In a series of experiments Sepri [18] and Chu [19] extended the surveys into the leading edge region as well as the downstream wake , and in another study from the same group Naranjit [20] investigated a circular body/wing combination.
More recently a series of experiments have been carried out at Imperial College concerning vortex boundary layer interaction in general. Shabaka and Bradshaw [21- 23] explored the flowfield around the leading edge and the junction extensively for turbulent flow , as was also done by Zamir & Young [13] for the turbulent version of their previous investigation.
McMachon et.al. [24-25] did Reynolds stress measurements in a configuration similar to the Shabaka-Bradshaw case, emphasizing the flow properties immediately upstream of and in the vicinity of the leading edge region. Khornilov and Kharitonov [26] have published a study addressing the question of the relative thickness of the two shear layers and its influence on the flow development. Hsing and Teng [27] studied another f simple wing combination both at low speeds and up to high subsonic Mach numbers, confirming that only moderate changes took place in the interaction up to Mach numbers of 0.8. The flow in the leading edge region is unsteady , and Rood [28 , 29] explored the effects of this unsteadiness downstream. for different profile nose radii. His measurements of the vortex pattern on both sides of a wing at incidence led to the conclusion that although the Kutta-Joukowski condition is fulfilled outside the boundary layer, it may not be fulfilled inside the flat plate boundary layer.This conclusion is contrary to the findings of Chu and Young [19] .
Devenport and Simpson [30] made a detailed investigation of the turbulence properties in the leading edge region. They used a circular protuberance and created a strong adverse pressure gradient downstream.
The leading edge of the junction has been the subject of several papers by Kubendran et.al. [31 , 32] . They show that with a proper filleting of the leading edge itself the strength of the vortex can be reduced dramatically.
Recently laser anemometry has been used for extensive documentation of , in particular , the leading edge region [33 - 35]. Abid and Schmitt [35] explored a local separation in the leading edge corner itself, confirming flow visualizations in the region. It is clear that it is necessary to use this type of non-intrusive measurement in wing/body junction flows , either as stand-alone measurements , but preferrably as a complement to other techniques, since other techniques for certain conditions may alter the flow field being measured. Mojola [36] has explored the probe interference problem, showing that massive changes in the flow pattern may result if interfering instrumentation is used in the leading edge vortex region.

As can be seen a large number of investigations have been performed to document the flowfields; the laminar and transitional may have relevance for practical cases on RPVs etc. , but the main interest for practical cases is information on turbulent junction flow.

In almost all the investigations above , a requirement of simplifying the geometry has led to the square corner interaction. It appears clear that the filleted cases existing on all aircraft , have not been explored properly. As the flow structure is complex , the design is most often left to the test engineer in charge of the project wind tunnel tests . The size of ' the coins in his pocket' determines the fillet radius. Scheiman and Kubendran [34] included some filleted data in their investigation . The main effect appears to be moving the vortex out from the corner and causing some local acceleration .

In the present paper two cases have been chosen to illustrate the flow occuring in realistic configurations; one is at full scale, flight conditions , while the other is a typical transport aircraft wind tunnel model:
• A filleted wing-fuselage junction (See Fig. 9) has been documented in flight for the main part of the subsonic Mach number regime, utilizing a variety of traditional and novel experimental techniques. This includes pressure rakes, static pressure taps , modified Preston tubes, rotating X-wires etc. The object was to determine the junction flow in a variety of conditions, ranging from close-to-separating boundary layer at low speeds up to transonic shocks occuring. It was clear that the stall of the aircraft was not caused by vortex breakdown, and the investigation therefore only concerns vortices developing under a moderately strong streamwise pressure gradient.
•Measurements have been made of mean and turbulent flow quantities in the wake of a wing/body junction of a typical transport aircraft model in the large European DNW tunnel's 6 x 8 meters test section. The main interest is here to see the possibilities of investigating this kind of complex flow on an ordinary development model of a new aircraft. Also in this investigation a major part of the information was obtained with the 5-probe x-wire rake discussed earlier.

WING BODY JUNCTION ON A SWEPT WING AIRCRAFT IN FLIGHT

Some results from the flight tests with the SAAB 32A Lansen aircraft are included in [37 and 38] , and in [39] some details of the wing/body junction flow were included.

In this investigation, just like in most wing/body junction flows , the crossflow is small. Hence , flow visualizations commonly used like tufts , oil-flow etc. provide little guidance. On the other hand it means that several "two-dimensional" techniques are feasible to use.

In the present case several technologies were utilized:
- pressure rakes on the fuselage upstream of the wing
- static pressure taps on the filleted surface
- a flat, movable surface mounted on the wing including static pressure taps
- modified Preston tubes [40 - 42] in the entire region
- pressure rakes , mounted on the wing
- 5-probe , X-wire rake , mounted on the wing
- dual hot-films

Figure 9 shows the geometry of the aircraft and the junction region; along with the coordinate system used for the junction. The spanwise coordinate starts at eta = 0.30 and runs perpendicular to the fuselage, along the wing , fillet and fuselage surface. The intersection wing/fillet and fillet/fuselage have been indicated in the figure. The fillet shape has been drawn for a series of boday stations and relative to a fuselage reference line. A more complete geometrical definition can be found in [37].

In the present paper the four different flow cases defined in [37] will be discussed:

Case	Mach	Altitude [km]
A	0.89	10
B	0.89	7
C	0.80	7
D	0.40	7

It is important to document the initial conditions for the interaction; i.e. measure the boundary layer properties upstream of and the pressure distributions in the region where the vortices form. Figure 10 shows sample velocity profiles and integral properties at a fuselage station slightly upstream of the wing, while Figure 11 shows how the wall pressure distribution in the interaction corner itself changes downstream.

The size of the junction region on the main wing has been illustrated in Figure 12 , where the static pressures and local skin friction have been plotted for three spanwise positions. Also shown in the Figure is the size of the interaction according to [8]. Bragg[11] suggested a formula for the interaction region size based on the friction velocity, suggesting that the effect on the wall shear should disappear at a distance based on the 2-D values of the friction velocity. Using his expression , the wall shear should attain undisturbed value for y+ = 2520 .Bragg's experiment was low speed. low Reynolds number flow, and the experience in the current experiment does not support his formulas. However, it appears that his general statement about and interaction size being 2*delta is reasonable. Using a panel method [43] coupled with a viscous code that includes a laminar integral method, empirical transition and separation bubble treatment and Bradshaw's [44] finite difference code for the turbulent boundary layer, the flow has been computed for the wing root in the absence of the fuselage. As can be seen the pressure distribution in this region corresponds to 0.5 degrees angle of attack rather than the 2 degrees geometrical angle for test case C.

Figure 13 shows spanwise distributions of pressure at 4 chordwise positions - note the repeatability for different flow cases at the upstream station. Also, it is clear that on the fillet itself very few traces can be found of the vortex pattern existing in the corner. While it would have been highly desirable to have pressure taps in the wing and fuselage part of the fillet , it was not possible due to the structural constraints in this part of the aircraft. Instead. , both static presure distribution as well as local skin friction was obtained through the use of modified Preston tubes. These are small (2 mm diameter) tubes taped onto the wing, fuselage and fillet surfaces, and the data presented here was obtained by shifting a set of modified Preston tubes to various spanwise positions over several flights.

Figure 14 shows the spanwise distribution of static pressure at several chordwise positions for one of the test cases. The corner region is clearly locatable here on the wing, with considerable spanwise pressure gradients. It is clear , that in the corner region itself there is a variation not only in velocity but also in static pressure over the entire three-dimensional flowfield. In most investigations this feature has not been addressed . In principle it might be possible to determine the distribution of static pressure from complementary measurements with , for example, total pressure probes and laser or carefully calibrated hot wires. However, the accuracy becomes poor, and we refrain from this procedure here. As an indication of the departures in static pressure present in the corner , data obtained using a static pressure tube on the boundary layer rake used for the total pressure measurements has been presented in Figure 15.

Local skin friction coefficients obtained with the modified Preston tubes are presented in Figure 16. The deviation from the wall shear distribution further out on the wing is clearly seen, with the kink in the distribution connected to the vortex in the flow field clearly visible. Although the resolution is not as good as might have been desired , the same features as described by , for example , Bragg [11] or Bradshaw[22] experimentally and Cousteix & Arnal [45] computationally, can be found. Towards the corner wing/fillet the wall shear is reduced , but there is an indication that the zero wall shear is actually displaced relative to the corner itself; this is indicated in the magnified plot of Figure 17 .

The same technique was used for the Preston tubes, was repeated with total pressure rakes, and samples of total pressure profiles are shown in Figure 18 . One general problem in this type of experiment, is that the rake itself might disturb the flowfield, and unlike traditional boundary layer flows , it is difficult to estimate the actual probe influence. Therefore , a technique was adopted where rakes of different size were used at the same location in different flights, thus having a control on both probe interference and repeatability. The results in Figure 18 are quite typical. At 22.5 % chord, the flowfield at one particular spanwise location in the vortex itself was measured with one rake 35 mm high and another 150 mm high. The results are very close , and indicate that the vortex pattern is correctly described with the instrumentation, it also seems that the features closer to the wall have some discrepancy.

The resulting isobar plot from measurements at several spanwise stations can be found in Figure 19. Results from several Mach numbers have been indicated , the low angle of attack, high Mach number cases involve a vortex pattern much smaller than the test case D (M = 0.4 , H = 7 km) that we dicuss mostly in the present paper. Figure 20 indicates what happens to the vortex as it moves downstream; it grows appreciably in size and moves out from the corner. Towards the rear of the junction, its effect on the wall flow is less pronounced , as has been seen in the distributions of static pressure and skin friction already. Note that the total pressure coefficient reaches zero for one part of the flow , corresponding to the total pressure itself being equal to the static reference pressure for the aircraft. The dynamic pressure is still high , though , due to the change in static pressure in the vortex.

A rake with 5 rotating X-wires were used to determine flow directions and measure turbulence in the current flow field. Analysis of hot-wire data in compressible flow is difficult, and to handle the present experiment , a special technique had to be developed. Briefly described it consists of measuring the time-averaged voltages from both wires on the sensor, at 12 different positions. Using the common response laws with a K-factor, the ratio of voltages for three different sets of data can be used to determine the magnitude and angular position of the cross-flow. As the K-factor for one particular wire at each particular Mach number or altitude is unknown , the three redundant sets of data (Figure 20) can be used to minimize the differences, and K is determined along with the flow angles. Thus , each sensor is reduced essentially as a single slanted wire, and by comparing the results from the two wires on the same sensor , it is possible to validate the determined flow angles. To obtain a true velocity information , it is necessary to use results from several Mach numbers, and comparing it with the total presssure measurements. It is clear, that this type of "calibration" can only be done with boundary layer flows, as the total pressure must be used to estimate the cross-flow. In Figure 21 a sample of results from different Mach numbers can be shown , demonstrating that the wire in this case seems to be fitted reasonably well with a King's law [46] approach. Having the K-factors determined and the constants A and B for the two wires in the probe , it is now possible to go back and reduce the time-averaged velocity vector and the turbulence characterisitics.

In the present paper we are concerned with the time-averaged cross-flow , and this could have been obtained in a much simpler fashion, as illustrated in the following Figures. In Figure 22 the results of plotting the voltage and voltage squared for a wire rotating 360 degrees is shown. The direction of maximum voltage can be found , and it is assumed that it coinsides with the direction of the crossflow vector. Figure 23 shows how the vector changes with Mach number for one rake position; the outer flow has a small, almost stationary variation , while the inner sensors are affected by the fact that the vortex moves through different parts of the flow field as the Mach number is change. Figure 24 illustrates the vectors for several spanwise positions for one particular flight condition.

It was stated earlier that the cross-flow in the wing body region was small , as the vortex did not separate the flow. At two spanwise positions , dual hot films ., Mc Croskey type [45] , were used to determine the local skin friction magnitude and direction using a technique described in [46]. Figure 25 shows how the measured cross-flow varied with flight conditions. It seems clear that cross-flow was smaller further out on the wing , and also that the cross-flow is too small to severely affect the readings of the modified Preston tubes. It can be seen that there is a change in flow pattern around M = 0.4. This indication by the hot films agrees with observations using other types of instrumentation on the entire wing, that the flow pattern changes at this Mach number. The leading edge bubble starts to break up on the outer part of the wing , causing a redistribution of wing loading and a corresponding change in crossflow. As the Mach number is decreased further , the separated area grows gradually from the outer part of the wing, until the entire wing is separated during stall.

TRANSPORT AIRCRAFT MODEL IN A WIND TUNNEL

Figure 26 illustrates the model geometry and the measurement areas. Two general areas were investigated ; one was the wake development downstream of the trailing edge , and the other one was a small region in a plane normal to the fuselage axis , immediately downstream of the trailing edge. Currently the data has been only partly analyzed , but Figure 27 indicates some of the features of this flow field.

CONCLUSIONS

It seems clear that a large number of experiments have been performed under laboratory condictions to document the flow in 90 degree interaction, be it laminar , transitional or turbulent. Both zero pressure gradients and pressure gradients leading to corner separations have been incvestigated. Also , computational approaches have been taken to compute the flows , ranging from simple, flat plate consideration to elaborate Navier-Stokes solutions. However , there seems to be a lack of detailed experiments for filleted cases , and it is hoped that the current flight experiment can be used for code development.
The flight experiments show that:

- The filleting of the leading edge and the junction leaves a vortex above the wing in the junction ; with the current instrumentation it has not been possible to verify the existence of , for example, a counterrotating vortex further up in the interaction region.

- Although the essential features of the flow interaction is similar to 90 degree corner interactions in laboratory experiments at low speeds, the filleting and the high Reynolds number in the presnt case, makes it

suitable as a test case for code development; this being despite the moderate resolution in some of the measurements.

• Measurements with the x-wire rake using redundant data, can be used for a fast and easy determination of three-dimensional crossflow. This iis particular useful in the wake region, as demonstrated by the wind tunnel model experiment.

REFERENCES

1. Roeder, J. : ' *Technologie im Airbus Programm. (Technology in Airbus* Programs.) ' Airbus Industries , 13. July , 1984.

2. Szodruch, J. , Hilbig,R. , Nitsche,W. and Olsson,J. : ' The role of experimental aerodynamics in future transport aircraft design.' AIAA Paper 87-1371 , June 1987.

3. Krenz, G. : ' Transonic Configuration Design.' AGARD Report No. 712 , May 1983.

4. Szodruch,J. : Integriertes Flügel- Antriebs System (Integration of wing-propulsion systems). Forschungsbericht W85-008 , German Ministry of Research and Technology , June 1985.

5. Fujii,K. and Obayashi,S. : ' Transonic flows over a wing-fuselgae combination.' AIAA Journal , vol. 25, no. 12 , pp. 1589-1596 , December 1987.

6. Bradshaw, P. : ' REVIEW - Complex turbulent flows.' Trans. ASME , J. Fluids Eng. , June 1975 , pp. 146-154.

7. Bradshaw, P. : ' Turbulent secondary flows. ' In: Annual Review of Fluid Mechanics, Vol. 19 ,1987 , pp. 53-74.

8. Gersten,K.: ' Corner Interference Effects.' DFL-Berict Nr. 108 (1959)

9. Carrier, G.F. ' The boundary layer in a corner' Q. Appl. Math. , Vol 4 , 1947 , pp. 367-370.

10. Tokuda, N.: ' Viscous flow near a corner in three dimensions.' J. Fluid Mech (1972) , vol 53 , part 1 , pp. 129-148.

11 Bragg, G.M. :' The turbulent boundary layer in a corner.' J. Fluid Mech (1969), vol 36 , part 3 , pp. 485-503

12. Young,A.D. : Some special boundary layer problems.' Zeitschrift für *Flugwissenschaften und Weltraumforschung.* 1 , (1977) , *Heft 6* , pp.401-414

13. Zamir,M. & Young,A.D.: ' Experimental investigation of the boundary layer in a streamwise corner.' Aeronautical Quarterly 21, (1970), pp. 313-339

14. Zamir, M. & Young, A.D. :' Pressure gradient and leading edge effects on the corner boundary layer.' Aeron. Quart. , August 1979, pp. 471-483

15. Barclay, W.H. : ' Experimental investigation of the laminar flow along a straight 135 deg corner. ' *Aeron. Quart.* 24 (1973), pp. 147-154

16. Mojola , J.J. and Young, A.D. : ' An experimental investigation of the turbulent boundary layer along a streamwise corner.' In: Turbulent Shear Flows. AGARD Conf. Proc. 93 (1971) , pp. 12.1-12.9

17. Mojola, O.O. : ' Empirical criteria for turbulent separation along a streamwise right-angled corner.' *J. Appl. Sci. Res., vol. 33, April 1977, pp.* 113-118.

18. Sepri,P. : ' An investigation of the flow in the region of the junction of a wing and a flat suface normal to the wing span.' Queen Mary College , E.R. 1002 (1973)

19. Chu, J.K. & Young, A.D. : ' A further investigation of viscous effects in a wing-plate junction.' Queen Mary College, E.R. 1003 (1975)

20. Naranjit, S.: ' An investigation of the flow over a wing-body combination,' Ph.D. thesis, University of London , 1976.

21. Shabaka , I.M.M.A. :' A preliminary experimental investigation of turbulent flow in a simplified wing-body junction.' Imperial College Aero Report 75-05 (1975)

22. Shabaka, I.M.M.A. & Bradshaw, P.:' Turbulent flow measurements in an idealized wing/body junction.' AIAA Journal 19,pp.131-132 (1981)

23. Mehta, R.D. , Shabaka, I.M.M.A. & Bradshaw, P. :' Imbedded longitudinal vortices in turbulent boundary layers.' In: Numerical and Physical Aspects of Aerodynamic Flows.(Ed. T. Cebeci) 1981

24. McMahon, H. , Hubbartt, J. & Kubendran, L. :' Mean velocities and Reynolds *stresses in a juncture flow.*' NASA CR-3605 (August 1982)

25. Kubendran,L. , McMahon,H.M. & Hubbartt, J.E. : ' Turbulent flow around a wing-fuselage type juncture.' AIAA Paper 85-0040. (1985)

26. Kornilov, V.I. & Kharitonov, A.M. :' Investigation of the structure of turbulent flows in streamwise asymmetric corner configurations.' Experiments in Fluids , 2 , 205-212 (1984)

27. *Hsing*, T.D. & *Teng*, H.Y. :' Experimental study of the behavior of 3D-turbulent boundary layer in a simplified wing/body junction.' AIAA Paper 84-1529 (1984)

28. Rood, E.P. : ' The separate spatial extents of the trailing horseshoe root vortex legs from a wing and plate junction.' AIAA Paper 84-1526 (1984)

29. Rood, E.P.: ' *The governing influence of the nose radius on the unsteady* effects of large scale flow in the turbulent wing and plate flow

30. Devenport, W.J. & Simpson, R.L.: ' Turbulence structure near the nose of a wing-body junction.' AIAA Paper 87-1310 (1987)

31. Kubendran, L.R. & Harvey, W.D.: ' Juncture flow control using leading-edge fillets.' AIAA Paper 85-4097 (1985)

32. Kubendran, L.R. , Bar-Sever, A. & Harvey, W.D. : ' Flow control in a wing/fuselage-type juncture. ' AIAA Paper 88-0614 (1988)

33. Meyers, J.P. & Hepner, T.E. : ' Velocity vector analysis of a juncture flow using a three-component laser velocimeter.' Presented at: 2nd International Symposium on Applications of Laser Anemometry to Fluid Mechanics , Lisbon, Portugal , July 2-4 , 1984.

34. Scheiman, J. & Kubendran,L.R. : ' Juncture flow measurements using laser anemometry. '. AIAA Paper 85-1612 (1985)

35. Abid, R. & Schmitt, R. : ' *Experimental study of a turbulent horseshoe* vortex using a three-component laser velocimeter.' AIAA Paper 86-1019 (1986)

36. Mojola,O.O. ' Measurements in a turbulent horseshoe vortex and the problem of probe interference'. Imperial College Aero Report 73-08 , December 1973.

37. Bertelrud, A.: ' Pressure distribution on a swept wing aircraft in flight.' In: AGARD AR-138 *Addendum* , 1984

38. *Bertelrud*,A. & Olsson,J.:' Method of analysing data on a swept wing aircraft in flight.' ICAS Paper 86-1.9.3, in 15th ICAS Congress Proc. 1986, London, England, September 1986.

39. Bertelrud,A.: 'The role of free flight experiments in the study of three-dimensional shear layers.' In: 'Perspectives in Turbulence *Studies*'. Ed.: H.U. Meier & P. Bradshaw, Springer Publ., 1987, pp. 250-299.

40. Preston,J.H. ' The determination of turbulent skin friction by means of *pitot tubes*' J. Ro Ae Soc , Vol 58 , 1954 , p. 109

41. Bradshaw, P. & Unsworth,K. ' A note on Preston tube calibrations in compressible flow.' Imperial College Aero Report 73-07 (1973)

42. Bertelrud, A.: ' Total head/static measurements of skin friction and surface pressure.' AIAA Journal , March 1977.

43. Kuethe, A.M. & Chow, C.Y.: ' Foundations of aerodynamics. Bases of *aerodynamic design.*' Wiley & Sons , 1986.

44. Bradshaw,P. , Mizner, G.A. & UNsworth,K.: ' Calculation of compressible turbulent boundary layers with heat transfer on straight-tapered swept wings.' Imperial College Aero Report 75-04 , 1974. See also: AIAA J. , Vol. 14 , 1976 , p. 399.

45. Cousteix,J. & Arnal,D. : ' *Turbulent flow in unbounded streamwise* corners (1).' in Three Dimensional Turbulent Shear Flows , St.Louis, Missouri, *June 1982. (AIAA/ASME Joint Conference)*

46. Doebelin , E.O. ' Measurement systems. Application and design.' McGraw-Hill (1966)

47. McCroskey,W.J. & Durbin,E.J.: ' Flow angle and shear stress measurements using heated films and wires.' J. Basic Eng. , Trans. ASME, March 1972, pp. 46-52

48. Bertelrud,A.: ' Use of hot film sensors and piezoelectric foil for measurement of local skin friction.' ICIASF '87 Record. Presented at 12th International Congress on Instrumentation in Aerospace Simulation Facilities, Williamsburg , Virginia, June 22-25 , 1987.

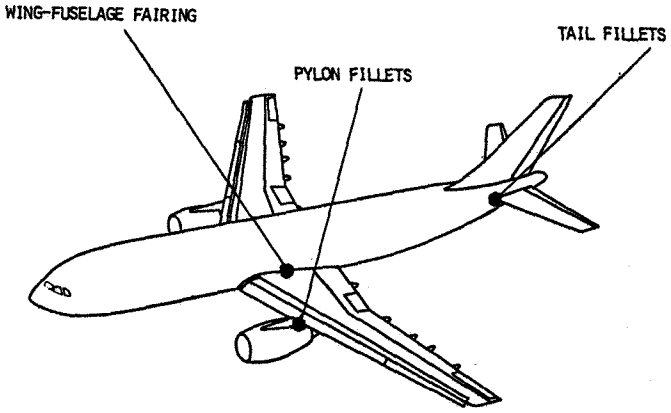

FIG.1 DRAG IMPROVEMENTS BY ADEQUATE FILLET DESIGN

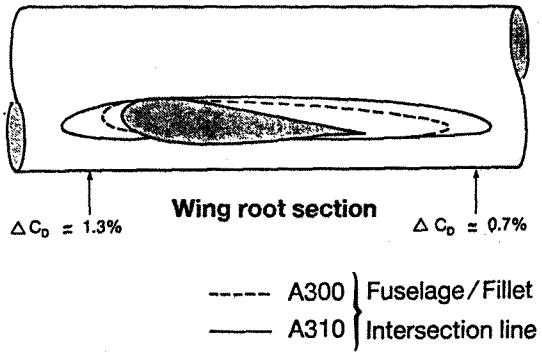

FIG.2 INTERFERENCE DRAG IMPROVEMENT AT WING-FUSELAGE

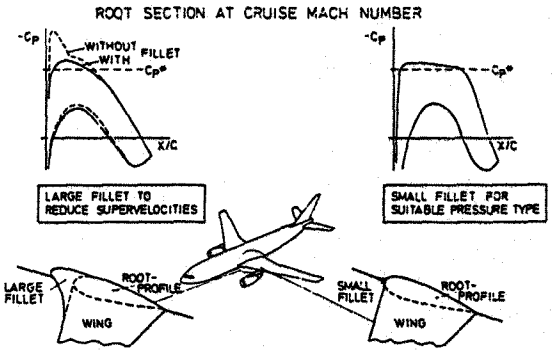

FIG. 3 Correlation of fillet size and pressure distribution [3]

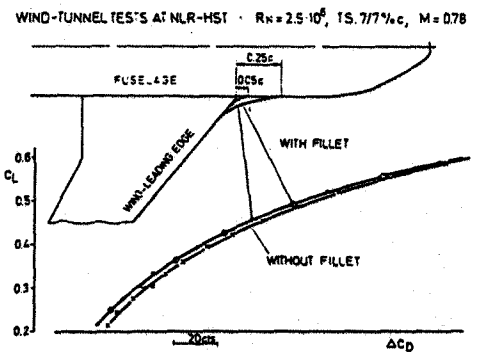

FIG. 4 Effect of wing-fuselage fillet on drag for a research wing of Airbus-type [3]

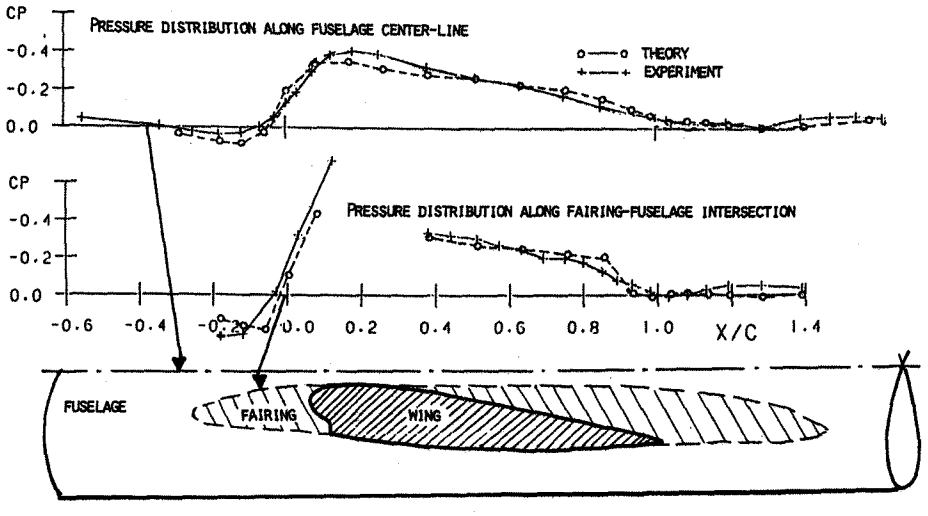

FIG.5 COMPARISON OF THEORETICAL AND EXPERIMENTAL PRESSURE DISTRIBUTIONS IN WING-FUSELAGE JUNCTIONS

M=0.82 , CL=0.65

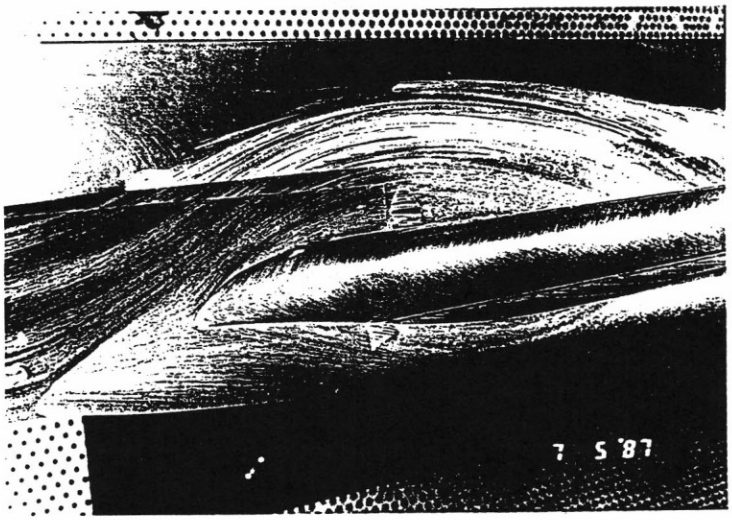

M=0.8 , CL=0.72

FIG.6 OIL FLOW VISUALIZATION IN WING-FUSELAGE JUNCTION OF A TRANSPORT AIRCRAFT

Figure 7 Interference Skin friction and displacement thickness. Zero pressure gradient. From Gersten [8]

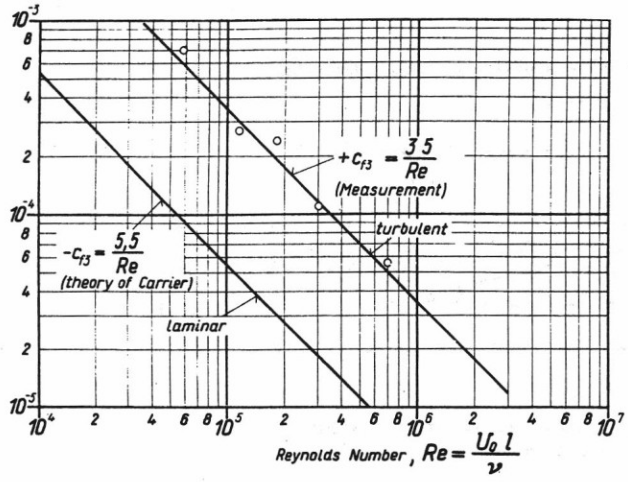

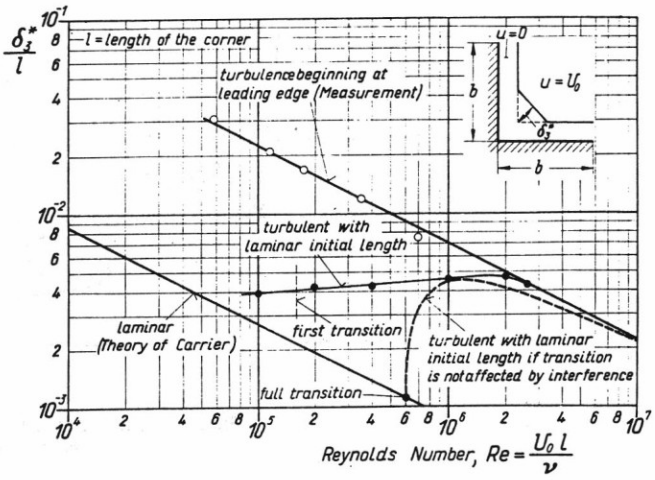

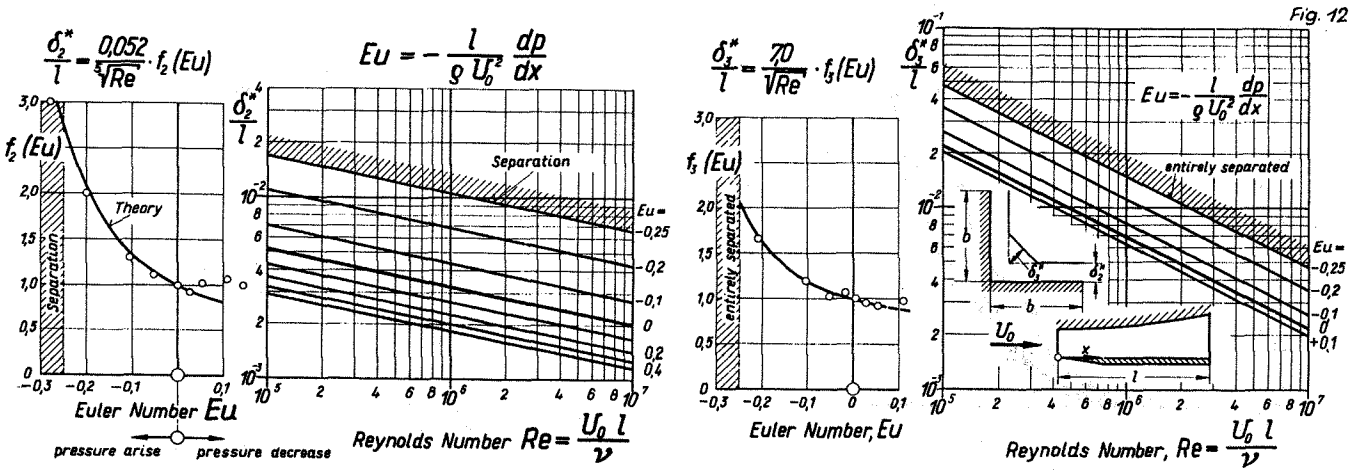

Figure 8 Flat plate and interference displacement thickness - pressure gradient effects. From Gersten [8]

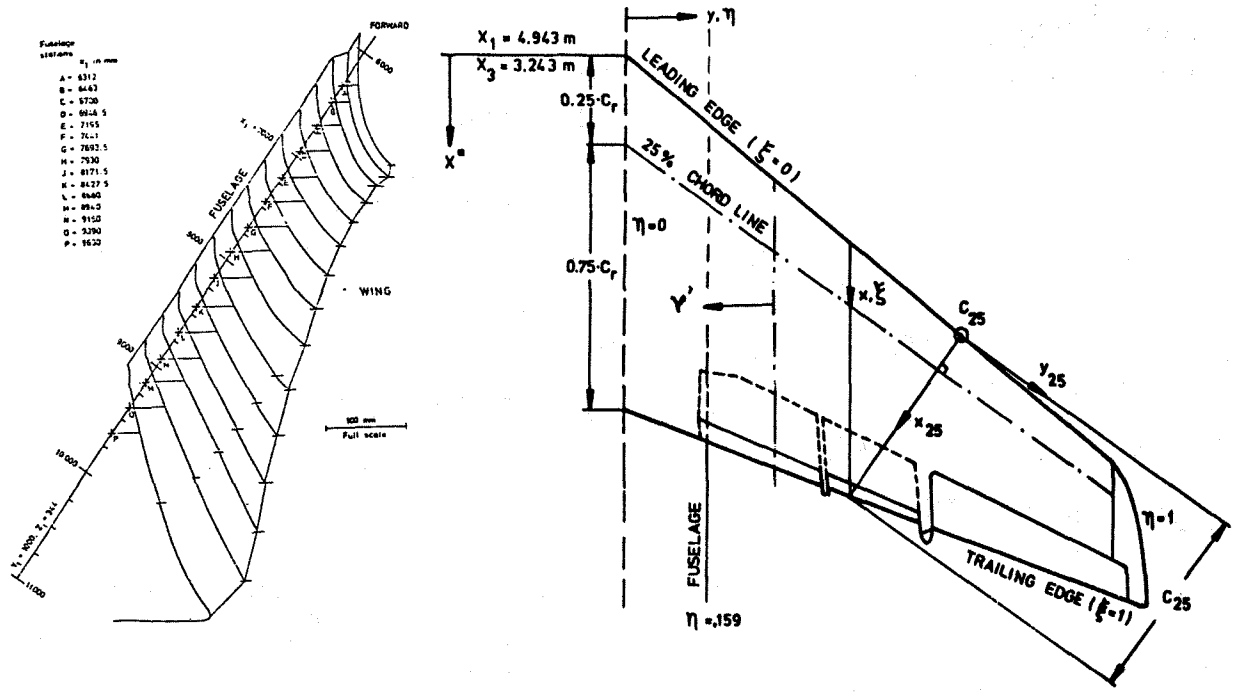

Figure 9 Wing body junction; fillet geometry and coordinate systems.

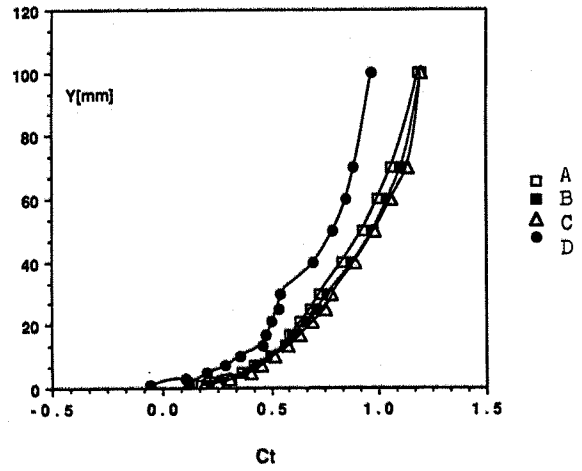

Figure 10 Fuselage boundary layer upstream of wing for four test cases. (Tape 106)

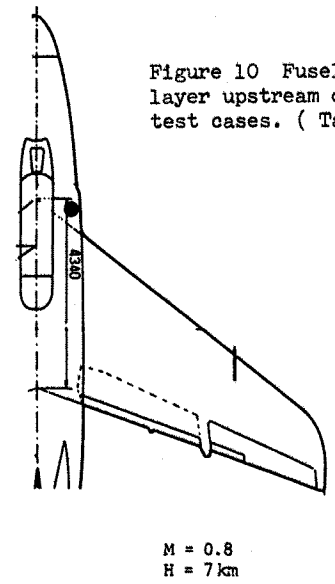

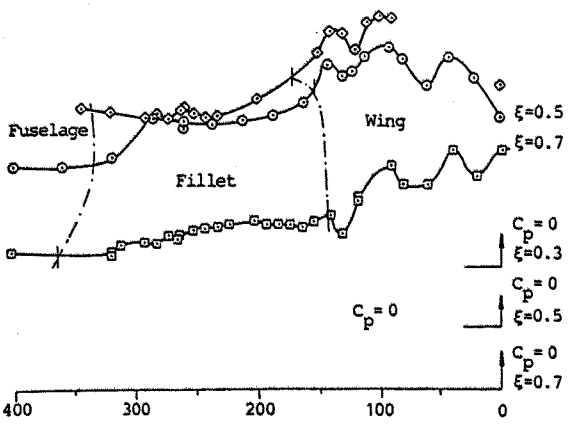

Figure 11 Spanwise pressure distributions, case C.

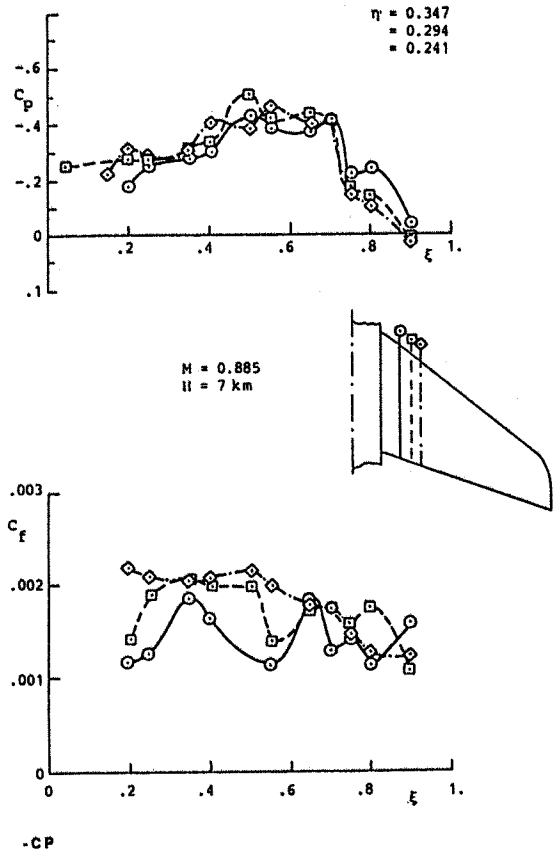

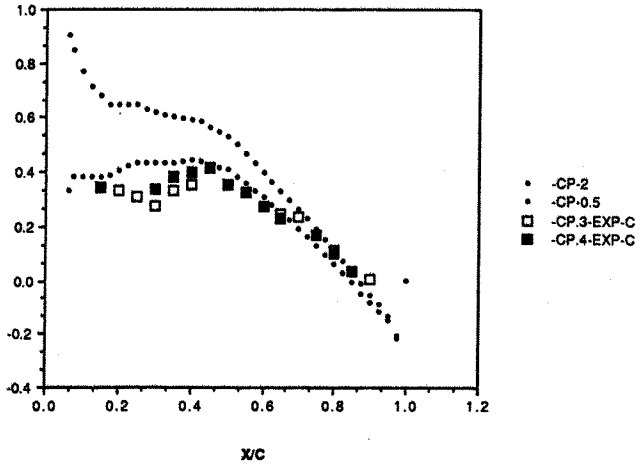

Figure 12 Coordinate distributions of static pressure and skin friction, case B. Computations and experiment from two spanwise stations, case C.

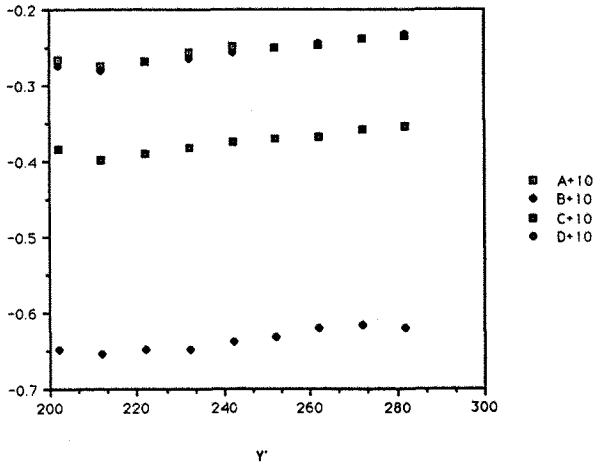

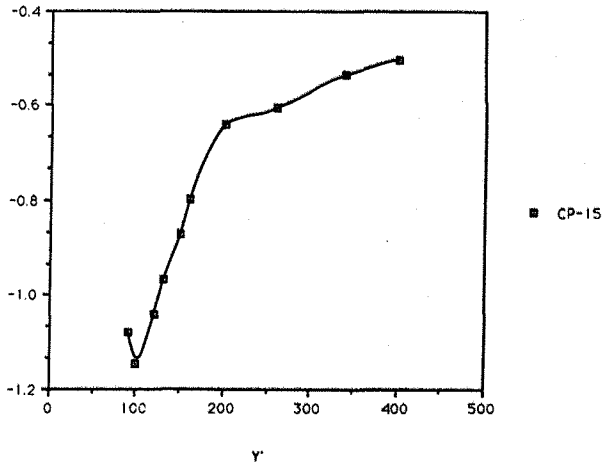

Figure 13 Spanwise pressure distributions for the four test cases, $\bar{x}/c = 0.1$

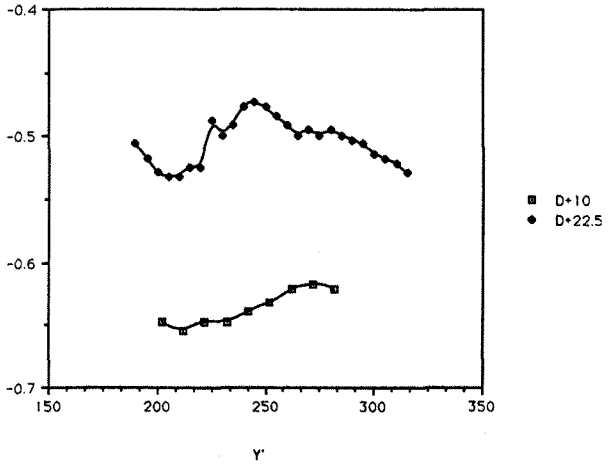

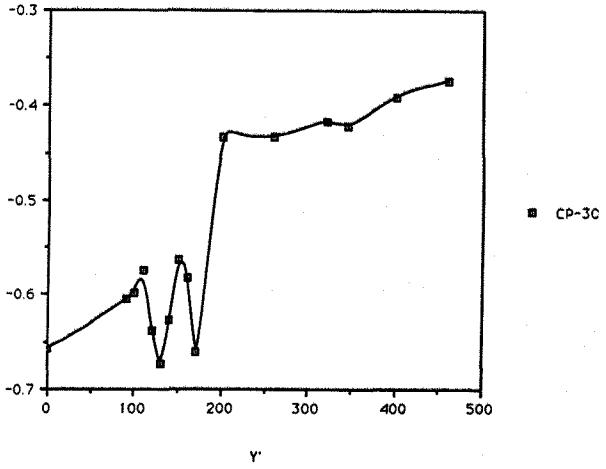

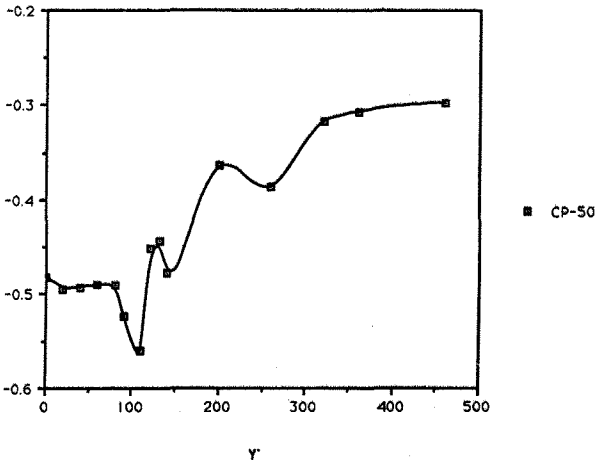

Figure 14 Spanwise pressure coefficients for test case D (M=0.4, H=7 km) at several chordwise positions :
- 10 and 22.5 % chord
- 15, 30 and 50 % chord

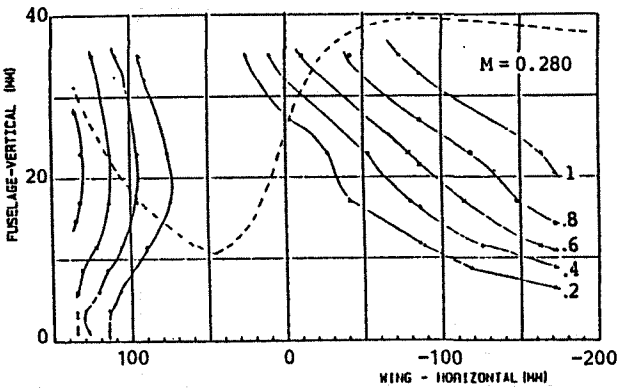

Figure 15 Static pressure (dashed line) in the flow field.

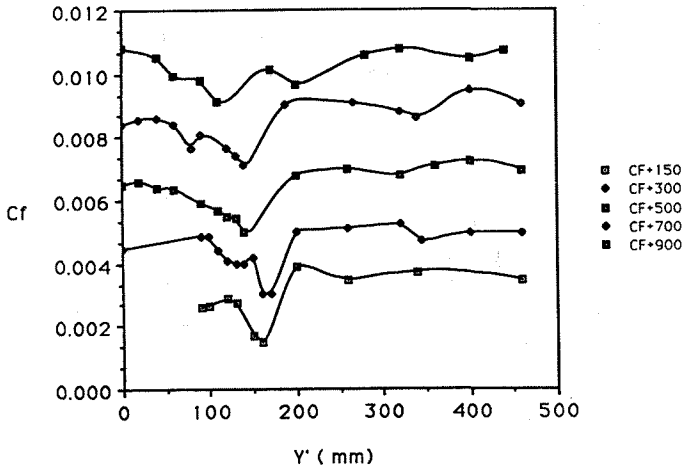

Figure 16 Spanwise distribution of local skin friction at 15, 30, 50, 70, and 90% chord. Note that curves are displaced. Test case D.

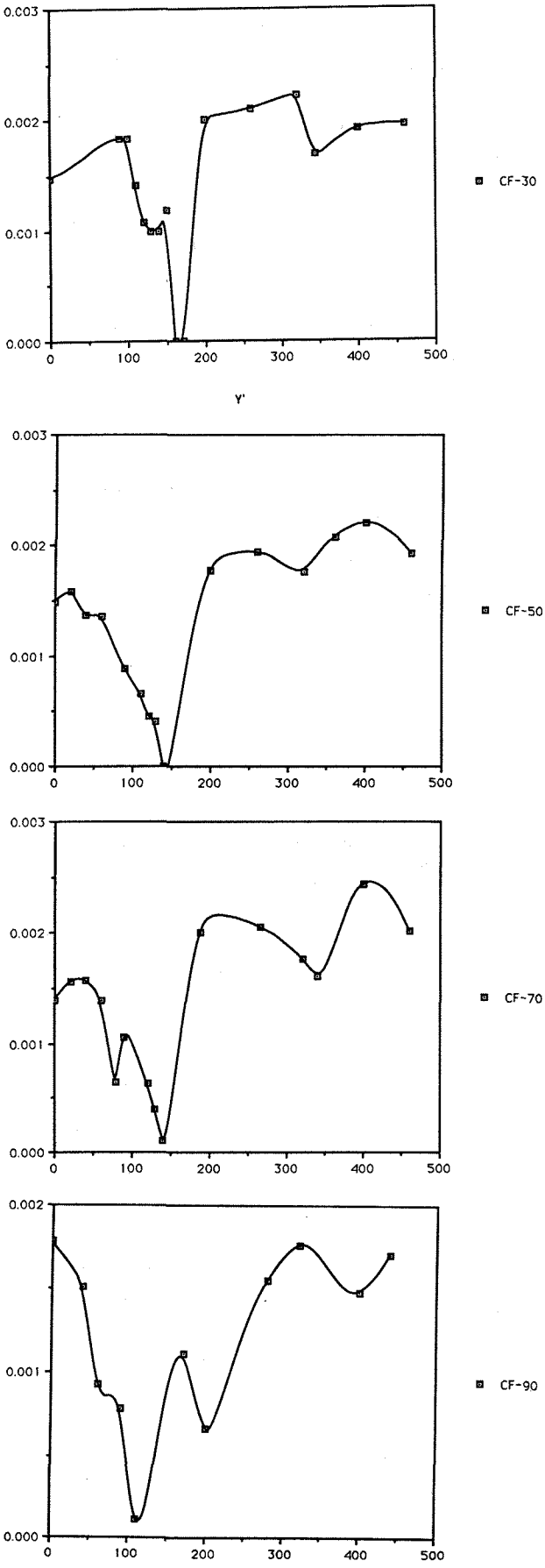

Figure 17 Magnified plot of spanwise distributions of local skin friction at 30, 50, 70, and 90% chord.

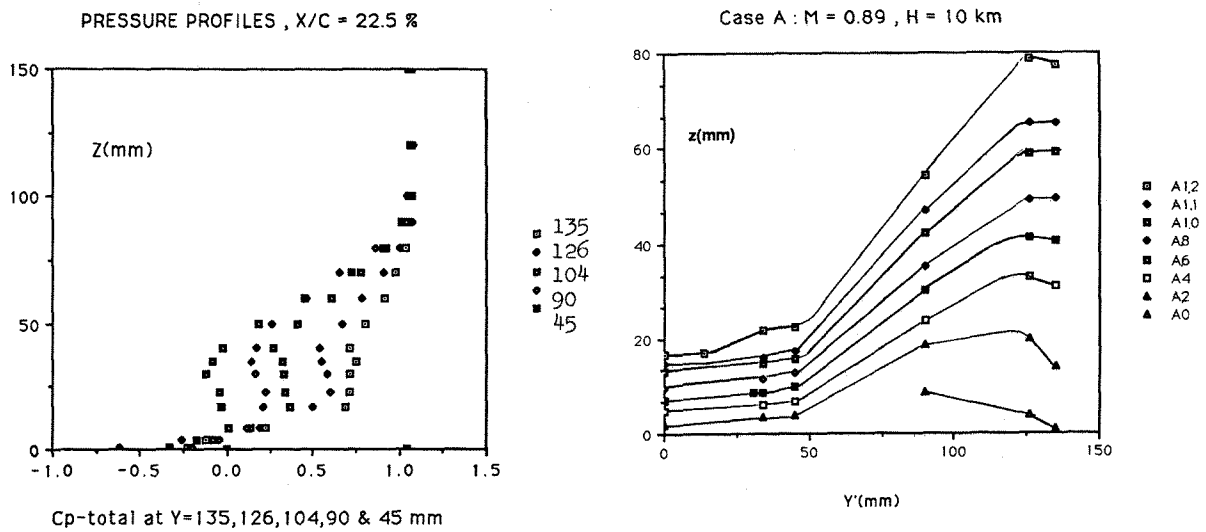

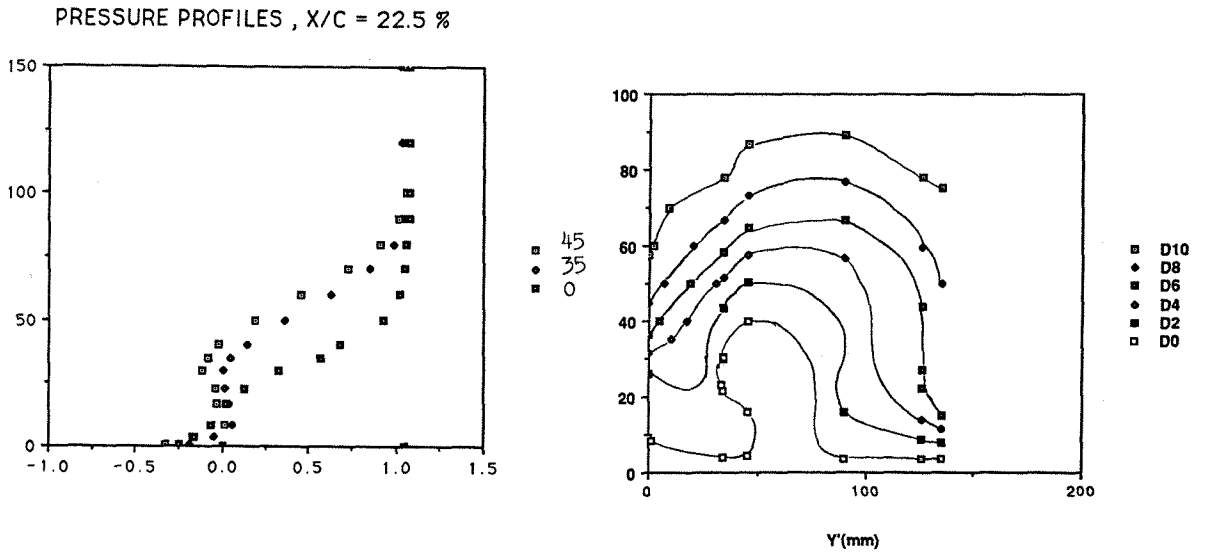

Figure 19_3 Isobar plots for several different Mach numbers at 22.5% chord. Note variations in vertical scale.

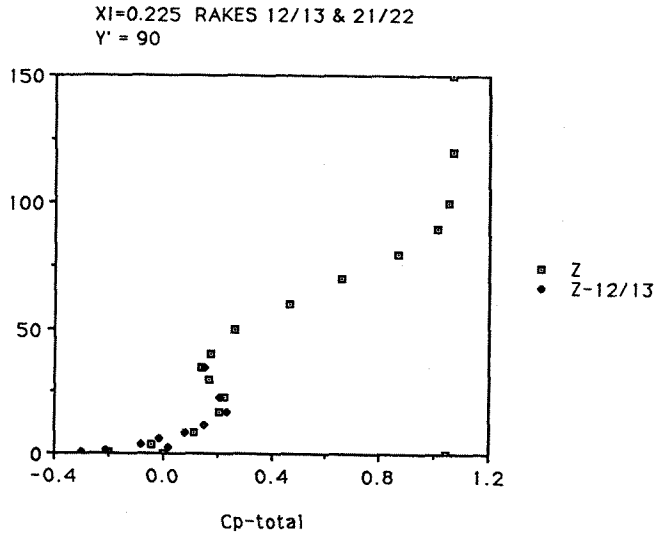

Figure 18 Total pressure profiles at 22.5% chord, test case D. Data obtained with two different rakes.

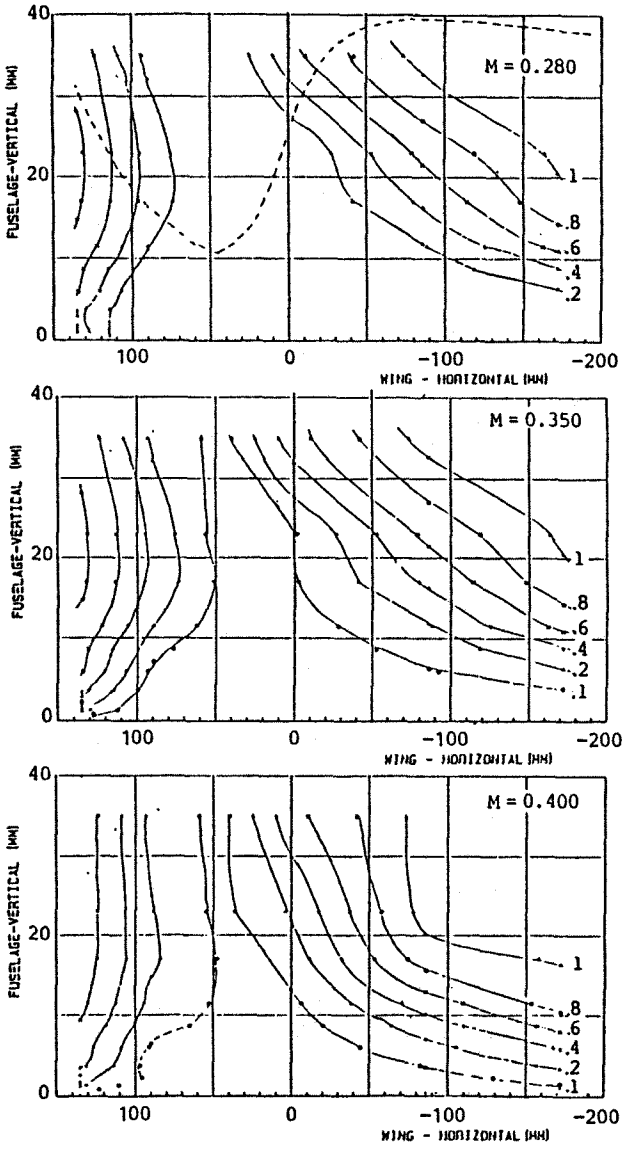

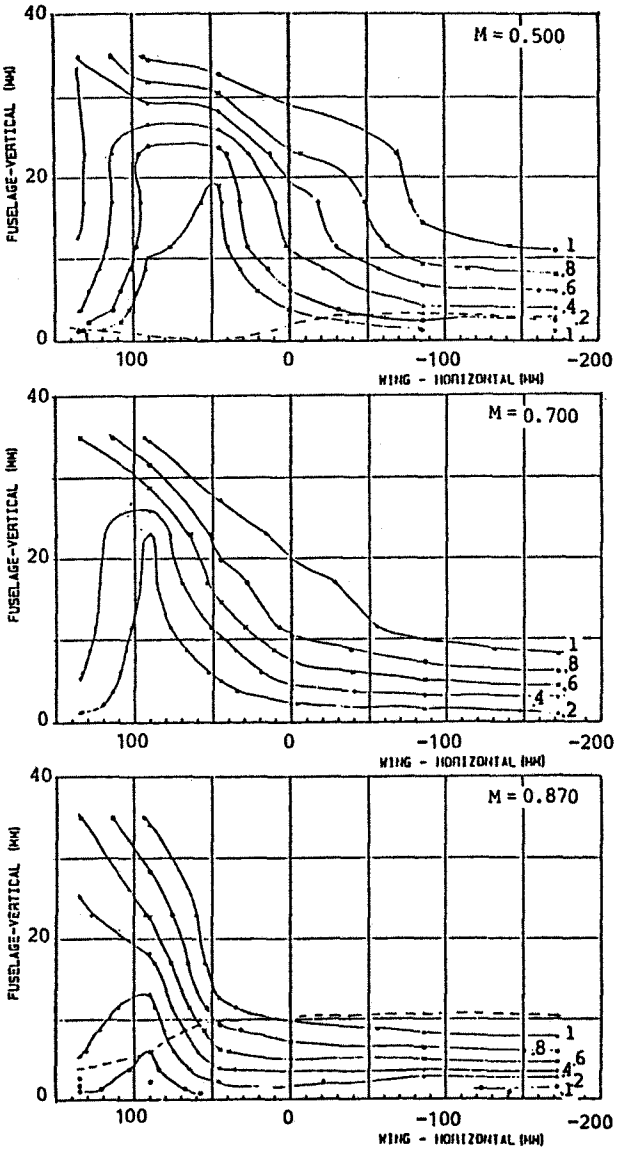

Figure 19b Isobar plots for several different Mach numbers at 22.5% chord. Note variations in vertical scale.

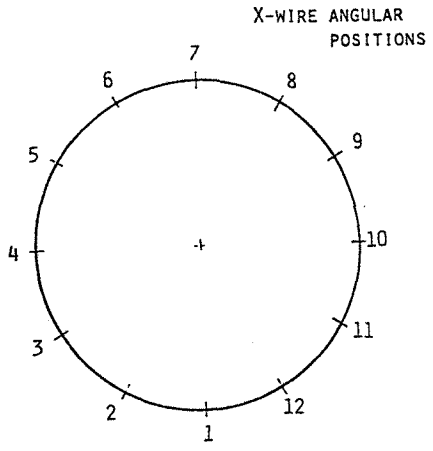

Figure 20 Principle of data reduction, using three redundant sets of data to determine K - factors.

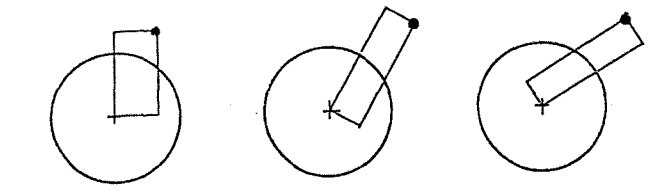

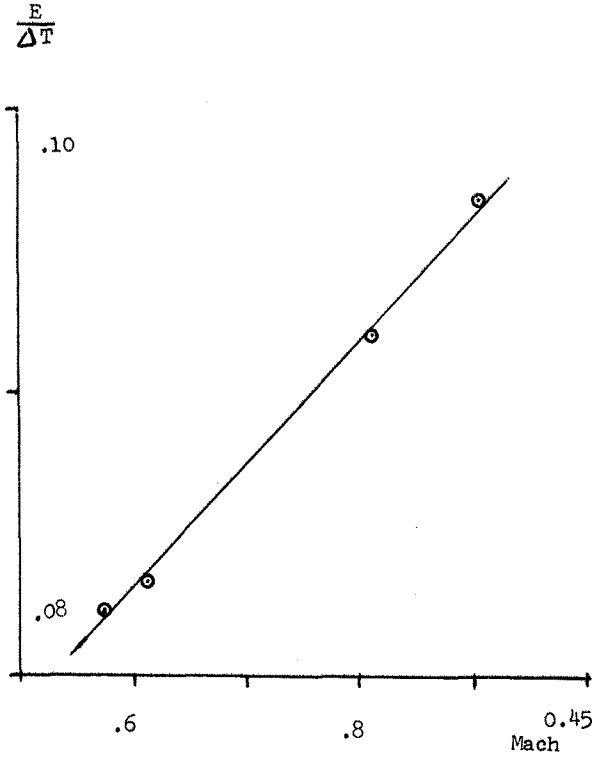

Figure 21 Heat flux versus Mach number for channel 5, Tape 121.

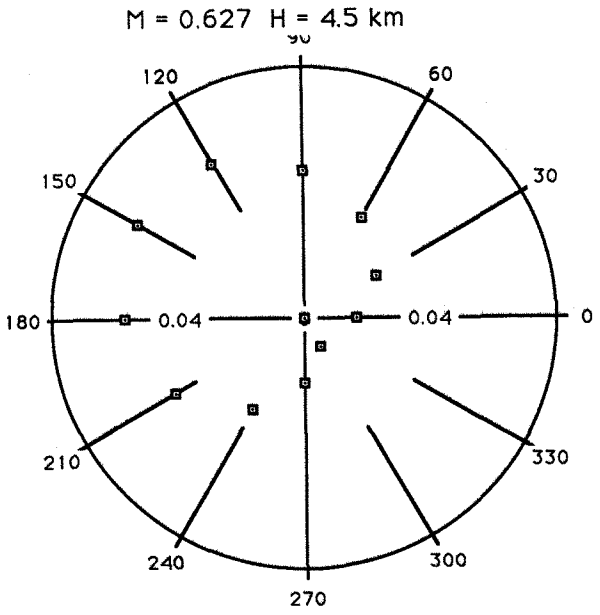

Figure 22 Voltage difference for various angular positions.

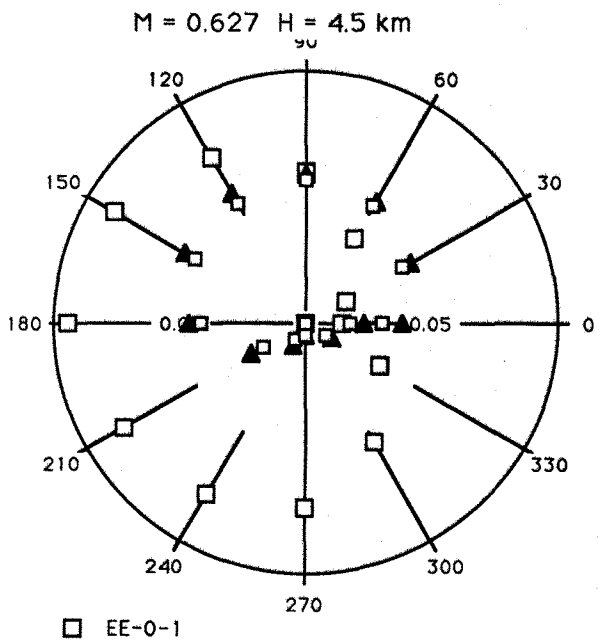

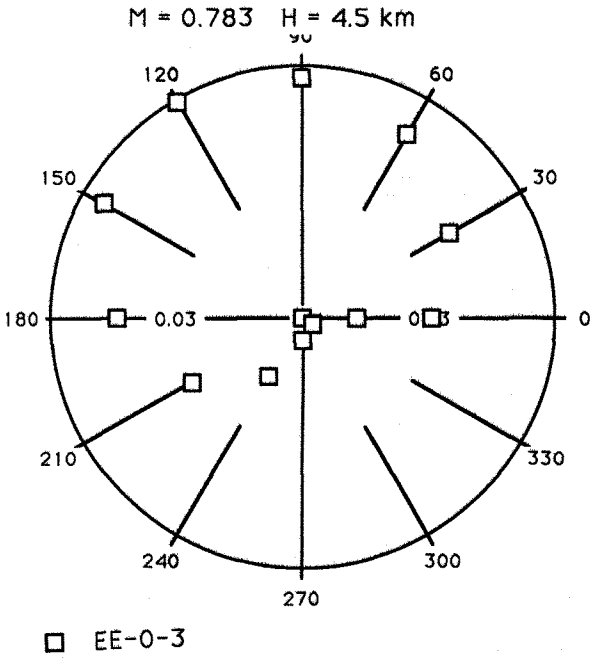

Figure 23 Flow vector at several Mach numbers.

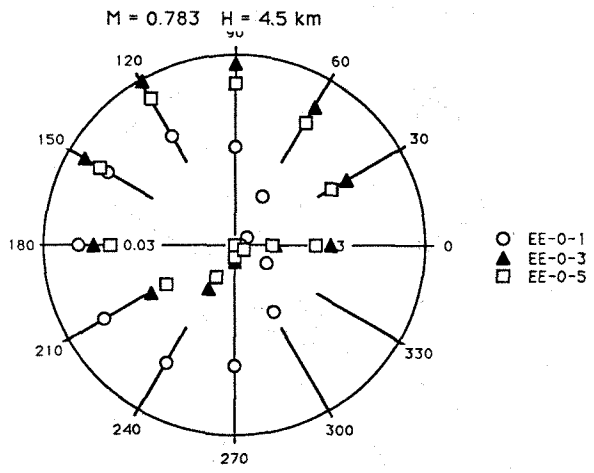

Figure 24 Flow vector at several spanwise positions.

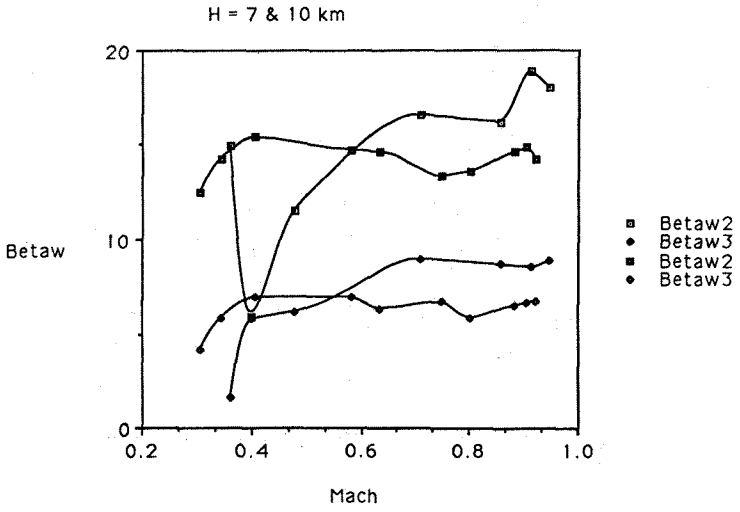

Figure 25 Cross-flow angle as function of Mach number.

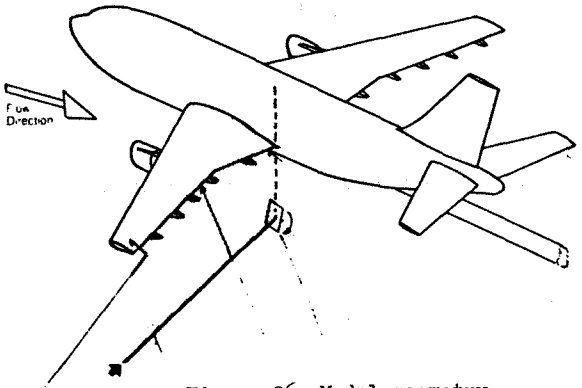

Figure 26 Model geometry.

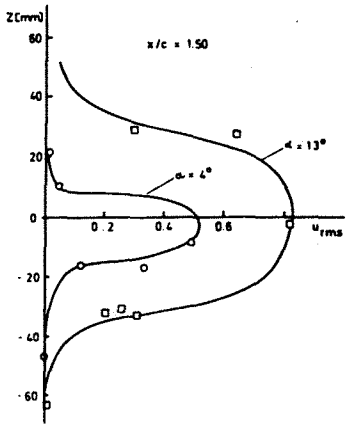

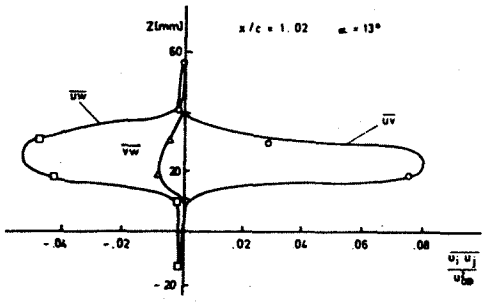

Figure 27 Sample of results.